Impulse response function analysis of pore pressures in earthdams

Stéphane Bonelli — Krzysztof Radzicki

Cemagref
Unité de Recherche Ouvrages hydrauliques et Hydrologie
3275 route de Cezanne, CS 400061
F-13182 Aix-en-Provence cedex 5
{stephane.bonelli, krzysztof.radzicki}@cemagref.fr

ABSTRACT. *In this paper, an Impulse Response Function Analysis (IRFA) method for analysing dam monitoring data is presented. The model developed, which was based on the approximation of the impulse response of the dam, gives the variations in the pore-pressure measurements resulting from changes in the reservoir and tailwater levels. An expression for explicitly estimating the* in situ *hydraulic diffusivity is presented. Analysis of monitoring data obtained at three dams establishes that with all the instruments used, the data obtained tend to show time lags with respect to the actual changes in the water level. The characteristic diffusion times were found to range between a few days and a few months. The results obtained here show that some essential aspects of the processes observed with most cells and piezometers data can be described in a linear framework and accounted for using this IRFA method with exponential decay.*

RÉSUMÉ. *Cet article présente une méthode d'analyse des mesures d'auscultation de barrages par réponse impulsionnelle. Le modèle reconstitue les évolutions des mesures de pression interstitielle en fonction du niveau du réservoir et du niveau aval. Une estimation de la diffusivité hydraulique* in situ *en est déduite. L'analyse des mesures d'auscultation de trois barrages montre que tous les instruments sont susceptibles d'avoir une réponse retardée par rapport aux évolutions de la retenue. Les ordres de grandeurs du temps caractéristique de diffusion sont de quelques jours à quelques mois. Les résultats obtenus démontrent que les phénomènes de base observés sur les cellules ou les piézomètres peuvent être décrits dans un cadre linéaire, et qu'ils sont reproduits par une exponentielle décroissante en temps.*

KEYWORDS: *seepage, impulse response function, earthdams, monitoring, time series.*

MOTS-CLÉS : *écoulement en milieu poreux, réponse impulsionnelle, barrages en terre, auscultation, séries chronologiques.*

DOI:10.3166/EJECE.12.243-262

1. Introduction

The tools most commonly used for dam monitoring data analysis purpose are the statistical methods of the Hydrostatic-Season-Time (HST) type. These methods were first developed in the 1960s to analyse the displacements resulting from the pendulum effects occurring at arch dams (Ferry and Willm, 1958; Willm and Beaujoint, 1967). They are still being used in several countries to analyse measurements of other kinds (Guedes and Coehlo, 1985; Silva Gomes and Silva Matos, 1985; Bonelli *et al.*, 1998; Carrère *et al.*, 2000).

The experience acquired at several hundreds of dams has confirmed what an excellent tool this approach can be for interpreting monitoring data. There seem to be no efficient methods available so far, however, in which the delayed effects are taken into account. Methods of this kind would make it possible to analyse hydraulic measurements.

The aim of this study was to draw up a useful model for interpreting pore-pressure measurements in and around dams, which are influenced by the reservoir and tailwater levels. This model was based on the Impulse Response Function Analysis (IRFA) of the dam works.

In the first section, it is proposed to discuss the weaknesses of the classical approach and to show the need for to take the time lags into account when analysing pore pressure measurements. The second part describes the approach used to model a linear parabolic problem, using an exact method of formulation based on Green's function and the approximation based on an exponential decay model. In the last part, this method of analysis is applied to monitoring data obtained at three dams.

2. The need for delayed response analysis

2.1. *Weakness of the Hydrostatic-Season-Time model*

The HST model is based on effects of three kinds. First there are the hydrostatic effects, which correspond to the variations H resulting from changes in the water level. This variable is given by a polynomial (which is often of the fourth order):

$$H(t) = b_1 z(t) + b_2 z^2(t) + b_3 z^3(t) + b_4 z^4(t) \qquad [1]$$

with $z(t) = (Z(t) - Z_{\min}) / (Z_{\max} - Z_{\min})$, where $Z(t)$ is the reservoir level, $Z_{\min}$ is the minimum level (that of the drainage blanket for example), $Z_{\max}$ is the maximum level (the height of the crest, or the normal reservoir operating level, for example). The second term is the time of year, which accounts for seasonal variations S in the measurements during twelve-month and six-month periods. This variable is given by the first two terms in the following Fourier series:

$$S(t) = A_1 \sin(\omega_a (t + d_1)) + A_2 \sin(2\omega_a (t + d_2)) \qquad [2]$$

where $\omega_a = 2\pi / \Delta T_a$ is the annual angular frequency (ΔT_a corresponds to a one-year period). The third term accounts for the time-dependent trends in the ageing processes. This variable can be expressed in various ways, depending on the process under investigation. It is often called the "irreversible effect".

This approach has been classically used to analyse dam monitoring data. It has also been used in many other fields (Young, 1998). One of its oldest known applications was developed by Forbes (1846) who used what he called the "sinusoidal adjustment method" to account for cyclic variations in the ground temperature. When applied to dams, this method is robust, and in most cases, it yields fairly satisfactory results. It has two main weaknesses, however:

1) the parameters involved have little mechanical relevance,

2) it does not take the specific structure of the time series analysed into account.

2.2. *Examples of delayed response measurements*

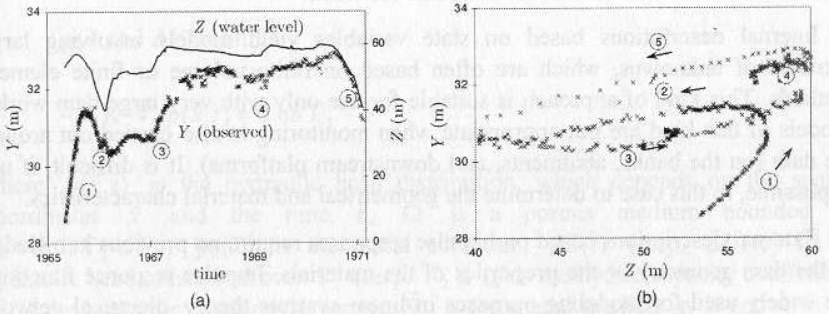

Figure 1. *Example of piezometer data: a) piezometric head vs. time, b) piezometric head vs. water level and hysteresis of a cyclic rise/drop in the water level*

Figure 1 gives an example of piezometric measurements carried out on the downstream toe of a dam. A priori, the variations occurring during the first few years of operation might be expected to be proportional to the reservoir level (Figure 1a), which would give a linear relationship between the piezometric values and the changes in the water level. This was not found to be the case, however (Figure 1b), and a polynomial of the type used in equation [1], even it is of an equally high order, would not account for these findings. Figure 1 shows how an increasing or decreasing cycle of change in the reservoir level has dissipative (hysteresis) effects. The trajectory differs depending on whether we are dealing with an increase (phase 3) or a decrease (phase 5). Some measurements can be taken to mean that an

increase in the interstitial pressure has occurred during a decrease in the reservoir level, and *vice-versa*. This well-known phenomenon has been observed *in situ* (Kjaernsli *et al.*, 1982; Myrvoll *et al.*, 1985) as well as being simulated under laboratory conditions (Windish and Høeg, 2000). The example shown below illustrates what is meant by delayed responses and shows why the model presented in equation [1] does not take these responses into account. We will return to this example later on.

2.3. *The need for an external means of description*

Dam monitoring data analyses usually deal with a large body of data and provide useful decision-making tools for assessing the safety of dams. These analyses have to be carried out periodically at short time intervals. In order to quantify the changes (i.e., the ageing) occurring under constant conditions, it is necessary in the first place to be able to account for any time-independent changes due solely to external constraints (such as variations in the reservoir and the precipitation levels). When dealing with dissipative processes, it is necessay to look at the loading history responsible for the levels occurring at a given moment, rather than simply taking the values of all the loads measured at the same moment.

Internal descriptions based on state variables yield models involving large numbers of unknowns, which are often based on finite volume or finite element methods. This kind of approach is suitable for use only with very large dam works. Models of this kind are not appropriate when monitoring is also carried out around the dam (on the banks, abutments, and downstream platforms). It is difficult, if not impossible, in this case to determine the geometrical and material characteristics.

External descriptions based on impulse responses require no previous knowledge of the dam geometry or the properties of the materials. Impulse response functions are widely used for modeling purposes in linear systems theory, electrical network theory, signal processing and control theory. Here it is proposed to use an approach based on the impulse response of the dam works: the Impulse Response Function Analysis (IRFA) method. The use of impulse response functions in a linear framework makes it possible to check a few well known properties: the principle of superimposition of loads, the stationarity, and the accommodation.

3. External modelling

3.1. *The linear description of seepage*

The pore pressure exerted by water seeping through a porous medium can be described by a parabolic equation. The description is taken here to be linear: dams can be assumed to behave in an approximately linear manner when they are in

normal operation. The main aim of this part of the present paper is to present a method of solving time-dependent linear parabolic problems in homogeneous materials. For the sake of simplicity, we will use the terms pore pressure, hydraulic head and piezometric level interchangeably, taking $p = z + u_w / \gamma_w$ to denote the hydraulic head, where z is the vertical elevation head, u_w is the pore water pressure and γ_w is the unit weight of water.

Let us look at the following linear parabolic problem:

$$c_v \frac{\partial p}{\partial t} - \vec{\nabla}_x \cdot (\mathbf{K} \cdot \vec{\nabla}_x p) = 0 \text{ in } \Omega \qquad [3]$$

with the initial condition

$$p(\vec{x}, 0) = p_0(\vec{x}) \text{ in } \Omega \qquad [4]$$

and the boy conditions

$$p(\vec{x}, t) = \Delta Z(t) \text{ on } \Gamma_1 \qquad [5]$$

$$p(\vec{x}, t) = \Delta V(t) \text{ on } \Gamma_2 \qquad [6]$$

$$-\vec{n} \cdot \mathbf{K} \cdot \vec{\nabla}_x p(\vec{x}, t) = 0 \text{ on } \Gamma_3 \qquad [7]$$

where $p(\vec{x}, t)$ is the hydraulic head distribution, which depends on the spatial coordinates $\vec{x}$ and the time t, Ω is a porous medium bounded by $\Gamma = \Gamma_1 \cup \Gamma_2 \cup \Gamma_3$, $p_0(\vec{x})$ is the initial condition, $\Delta Z(t)$ (resp. $\Delta V(t)$) is the hydraulic head prescribed over Γ_1 (resp. Γ_2), c_v is the hydric capacity coefficient, $\mathbf{K}$ is the hydraulic conductivity tensor, $\vec{\nabla}_x$ is the spatial gradient in $\vec{x}$ and $\vec{n}$ is the outward unit vector normal to Γ. To simplify, it is assumed that the initial condition fulfils the initial boundary conditions.

In terms of the Green's function $g(\vec{x}, \vec{x}', t)$ associated with problem [3]-[7], the solution is defined by:

$$p(\vec{x}, t) = p_0(\vec{x}) + h_0(\vec{x}, t, p_0) * u(t) + h_1(\vec{x}, t) * \Delta Z(t) + h_2(\vec{x}, t) * \Delta V(t) \text{ in } \Omega \qquad [8]$$

with

$$h_0(\vec{x}, t, p_0) = -\int_\Omega p_0(\vec{x}') \frac{\partial g(\vec{x}, \vec{x}', t)}{\partial t} d\vec{x}' \qquad [9]$$

$$h_1(\vec{x},t) = -\int_{\Gamma_1} \vec{n}(\vec{x}') \cdot \mathbf{D} \cdot \vec{\nabla}_{x'} g(\vec{x},\vec{x}',t) d\vec{x}' \qquad [10]$$

$$h_2(\vec{x},t) = -\int_{\Gamma_2} \vec{n}(\vec{x}') \cdot \mathbf{D} \cdot \vec{\nabla}_{x'} g(\vec{x},\vec{x}',t) d\vec{x}' \qquad [11]$$

where $\mathbf{D} = c_v^{-1}\mathbf{K}$ is the diffusivity tensor, $u(t)$ is the Heaviside step function, and the operator "$*$" is the time convolution product.

This approach is based on a well-established theory (Roach, 1970; Beck *et al.*, 1992). Equation [9] amounts to an external description, where h_0 is the impulse response to the initial condition $p_0(\vec{x})$ in Ω, and h_1 (resp. h_2) is the impulse response to the Dirichlet condition ΔZ on Γ_1 (resp. ΔV on Γ_2). In real-life cases, the Green's function is unknown. An alternative method which is classically used in the field of signal processing, consists in constructing models for these impulse response functions $h_i(\vec{x},t)$, which are at least approximately valid.

3.2. *External representation using an exponential decay model*

The simplest approximation for the impulse response function [9]-[11] is given by the exponential decay:

$$R(t,\alpha,\eta) = \frac{\alpha}{\eta} e^{-\frac{t}{\eta}} u(t) \qquad [12]$$

The variations attributable to the loading a_j (of either the Dirichlet or Neumann type) can be approximated using the model [12] as follows:

$$P_j(\vec{x},t) = R\left[t,\alpha_j(\vec{x}),\eta_j(\vec{x})\right] * a_j(t)$$

where $(a_0,a_1,a_2) = (u,\Delta Z,\Delta V)$, and $j \in \{0,Z,V\}$. The solution $p(\vec{x},t)$ is finally approximated by:

$$P(\vec{x},t) = p_0(\vec{x}) + \sum_{j\in\{0,Z,V\}} P_j(\vec{x},t) \qquad [13]$$

The advantage of approximation [13] is that we have located the description. All the information about the spatial structure of the solution is contained in the fields $\{\alpha_j(\vec{x}),\eta_j(\vec{x})\}_{\vec{x}\in\Omega}$. If the latter are known, it will be possible to model the changes with time in the field $\{P(\vec{x},t)\}_{\vec{x}\in\Omega}$. To model the time-related changes in $P(\vec{x}^*,t)$ at a single given point $\vec{x}^*$ (that of the measuring instrument), it suffices to determine $(\alpha_j(\vec{x}),\eta_j(\vec{x}))$. It is not necessary to specify $P(\vec{x},t)$ at other points in the field as

required by local methods of the finite volume or finite elements kind. This property makes the external approach particularly suitable for analysing time series. There is no need to describe the geometry of the boundary problem explicitely by meshing it. However, the main disadvantage of this method is that the parameters are liable to be less mechanically relevant.

Coefficient $\alpha_j(\vec{x})$ is equal to the value of $p(\vec{x},t)$ under permanent dam operating conditions if the sole non-null load a_j is a unit step. Coefficient $\eta_j(\vec{x})$ is a characteristic diffusion time: the system has some memory of the previous values of the loading time series. The role of this parameter is given by the following harmonic analysis:

$$R(t,\alpha,\eta) * \sin(\omega t) = g\sin(\omega t + \phi)$$

where $g = \alpha/[1+(\omega\eta)^2]^{1/2}$ is the damping coefficient, and $\phi = -\text{atan}(\omega\eta)$ is the phase lag corresponding to a harmonic load with temporal frequency ω. Under slowly varying loading conditions ($(\omega\eta)^2 = 1$), one obtains $g \approx \alpha$ and $\phi \approx -\omega\eta$. The characteristic time η therefore gives the time elapsing between the onset of the loading and the response, and α characterises the damping.

3.3. *Some IRFA models for pore pressure analysis*

The time origin $t = 0$ is taken to be a relevant date between the completion of the dam and the moment when it begins to be filled for the first time. During the first years of dam operation, the hydraulic head is assumed to be influenced by:

– the initial state of the dam, with a characteristic time η_0;

– the reservoir water level $\Delta Z(t) = Z(t) - Z_{\min}$, with a weighting coefficient α_Z and a characteristic time η_Z;

– the tailwater level $\Delta V(t) = Z_{tw}(t) - Z_{\min}$, with a weighting coefficient α_V and a characteristic time η_V, where $Z_{tw}(t)$ is the tailwater level measured;

– the pluviometry $Q(t)$, the formulation of which is beyond the scope of the present paper.

The corresponding IRFA model, which is suitable for analysing data obtained during the first few years of dam operation, will have the following general form at the given point $\vec{x}$ (which has been omitted for the sake of simplification):

$$P(t) = p_0 e^{-\frac{t}{\eta_0}} + \frac{\alpha_Z}{\eta_Z}\int_0^t \Delta Z(t') e^{-\frac{t-t'}{\eta_Z}} dt' + \frac{\alpha_V}{\eta_V}\int_0^t \Delta V(t') e^{-\frac{t-t'}{\eta_V}} dt' + Q(t)$$

It emerges quite clearly that we are dealing with a non stationary process, namely the dissipation of the initial pore pressures p_0. This process can be taken to be

irreversible and non stationary, but it can by no means be assimilated to a drift or an ageing process.

The second model is suitable for analysing monitoring data collected when the dam is operating, starting at a sufficiently long date t_0 after the dam was first filled ($t_0 \gg \eta_0$) for the influence of the initial pore pressures to be negligible:

$$P(t>t_0) = c + \frac{\alpha_Z}{\eta_Z}\int_0^t \Delta Z(t')e^{-\frac{t-t'}{\eta_Z}}dt' + \frac{\alpha_V}{\eta_V}\int_0^t \Delta V(t')e^{-\frac{t-t'}{\eta_V}}dt' + Q(t) + T(t) \qquad [14]$$

where c is a constant, and where the explanatory variable $T(t)$ accounts for the other non stationary effects (such as ageing), the formulation of which is beyond the scope of the present paper.

3.4. *The temporal moment matching method*

A direct identification procedure can be carried out by specifying (α_j, η_j), taking the first temporal moments of h_j and R_j to be equal at any $\bar{x}$: this is the temporal moment matching method. The order-k temporal moment of $a(\bar{x},t)$ is

$$M_k[a](\bar{x}) = \int_0^\infty t^k a(\bar{x},t)dt \qquad [15]$$

We take $\hat{a}(s)$ to denote the Laplace transform of a time-varying function $a(t)$. The Taylor-Lagrange development of $\hat{a}(s)$ around $s=0$ is

$$\hat{a}(s) = M_0[a] - M_1[a]s + o(s^2)$$

The moment matching method applied to $\hat{R}$ and $\hat{h}$ therefore consists in equalizing the first coefficients in the power series expansion for $\hat{R}$ and $\hat{h}$. However, as $\hat{h}\to 0$ and $\hat{R}\to 0$ when $s\to\infty$, the result of the identification is more accurate than obtained by performing a simple identification on the two coefficients in the power series. For further details about temporal moments, see Goltz and Roberts (1987) or Delay *et al.* (1998). In the present case, we obtained:

$$\alpha_j(\bar{x}) = M_0[h_j](\bar{x}),\ \eta_j(\bar{x}) = \frac{M_1[h_j](\bar{x})}{M_0[h_j](\bar{x})} \qquad [16]$$

This identification procedure can be used to make the parameters mechanically significant. However, it naturally requires determining the Green's function.

3.5. *A representative one-dimensional problem*

Let us consider the following one-dimensional problem:

$$\frac{\partial p}{\partial t} - D\frac{\partial^2 p}{\partial x^2} = 0,\ 0<x<L,\ t>0 \qquad [17]$$

$$p(x,0) = p_0(x),\ 0<x<L \qquad [18]$$

$$p(0,t) = \Delta Z(t),\ p(L,t) = \Delta V(t),\ t>0 \qquad [19]$$

The Green's function of this problem can be written using classical results (Morse,1953; Beck *et al.*, 1992; Melnikov, 2000):

$$g(x,x',t) = \frac{u(t)}{2L}\left[\theta_3\left(\frac{\pi(x-x')}{2L}, e^{-\pi^2 t/T}\right) - \theta_3\left(\frac{\pi(x+x')}{2L}, e^{-\pi^2 t/T}\right)\right] \qquad [20]$$

where $T = L^2/D$ is the characteristic diffusion time, and θ_3 is the elliptic function of the third kind (Gradshtein, 1980). Substituting from [10], [11], [15], [16] and [20], the temporal moment matching method yields the following closed-form results:

$$\alpha_Z(x) = 1 - \frac{x}{L},\ \eta_Z(x) = \frac{T}{6}\left[1-\alpha_Z(x)^2\right] \qquad [21]$$

$$\alpha_V(x) = \frac{x}{L},\ \eta_V(x) = \frac{T}{6}\left[1-\alpha_V(x)^2\right]$$

3.6. *Mechanical significance of the parameters*

The problem solved in [17]-[19] can serve as an illustration. It is similar to that arising, if one simplifies the geometry, in a homogeneous earthfill dam or in the core of a zoned dam. Initial pore pressures $p_0(x)$ result from the layered method of construction used. The water level $\Delta Z(t)$ varies at the upstream face. The tailwater level $\Delta V(t)$ occurs downstream. The results given in [21] can be interpreted in mechanical terms. This is the case in particular when the measuring instruments are located in an earthfill dam or in the core of a dam area. The length L can be said to correspond to the mean seepage path between the loading point (the upstream face), and the outlet point (chimney drain, drainage blanket, downstream face) (Figure 2).

The static damping coefficient α_Z contains information of two kinds:

– about the efficiency of the drainage system (vertical drain, drainage blanket, pressure relief pipes) or the sealing systems (grout curtain);

– about the position of the measuring instrument on the seepage path with respect to the upstream face of the dam in a homogeneous dam (Figure 2a), or to the upstream face of the core in a zoned dam (Figure 2b).

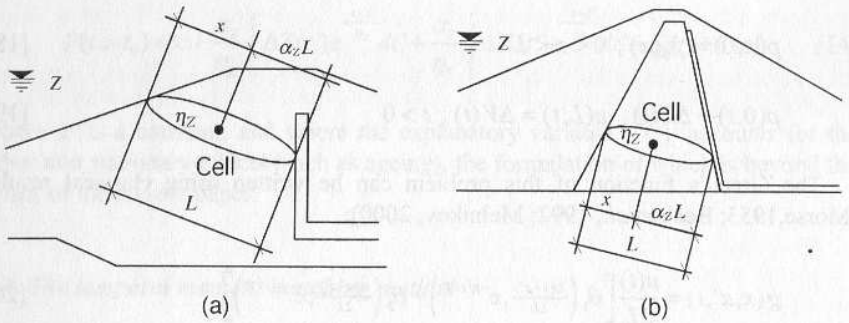

Figure 2. *Interpretation of parameters α_Z (relative distance from the measurement point to the drainage system), η_Z (characteristic response time of the measurement point) and L (mean length of the seepage path): a) homogeneous earthdam, b) zoned earthdam*

The characteristic time of the local effects of the water level η_Z contains information of two kinds:

– about the efficiency of the drainage system, in terms of the square of L;

– about the diffusion coefficient D of the area in which the measuring instruments are installed.

A coefficient α_Z around the unit value means either that the instrument is located near the upstream face (and x is small) or that the outlet point is located far from the loading point (and L is large). A very large time η_Z will reflect the presence of either a highly impermeable soil or a very long seepage distance L. A non-null time η_Z will reflect a non-null capacity.

The characteristic time η_Z makes it possible to assess the mean diffusion coefficient if L is given. An expression can be derived using [21]:

$$D = \frac{(1-\alpha_Z^2)L^2}{6\eta_Z} \qquad [22]$$

This diffusivity is estimated in one-dimensional terms with simplified conditions (as regards the homogeneity and isotropy, in particular). These assumptions are local. They relate only to the zone under investigation, which is that located between

the upstream and downstream faces. However, this simplified identification procedure based on the moment matching method does not call into question the validity of the IRFA method.

4. Applications

In this section, the exponential decay IRFA method is applied to dam monitoring data. The Levenberg-Marquart method was used to minimise the mean square error between the measurements $Y(\vec{x},t)$ and the model $P(\vec{x},t)$ at a given point $\vec{x}$ during a suitably chosen time interval.

4.1. *Application to a homogeneous earthdam*

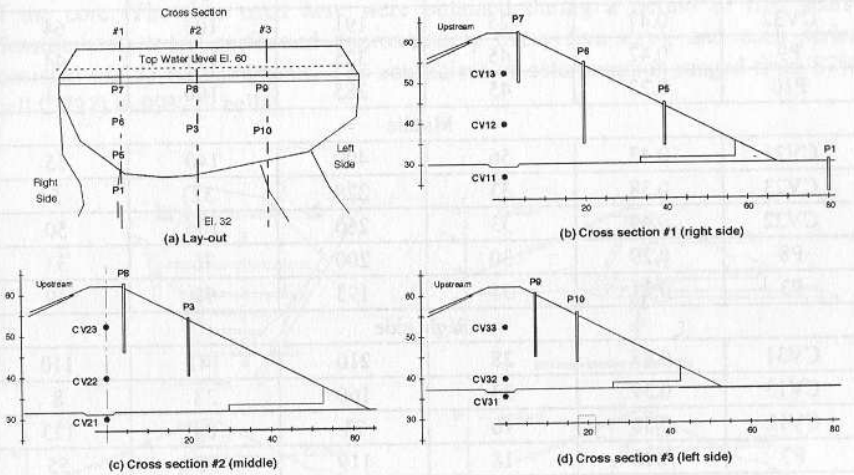

Figure 3. *Dam no.1, lay-out, cross-section locations, piezometer and pore-pressure cell locations*

The measurements obtained on a homogeneous earthfill dam 30 m in height with a horizontal drainage blanket were analysed. This dam will be referred to as dam no.1. The model in [14] was used, without taking the effects of the rainfall, the effects of the ageing, or the effects of the tailwater level into account, as they were negligible. The body of the dam was made of sandy clay with a permeability ranging between 10^{-5} and 10^{-7} m/s. The downstream slope was monitored using seven piezometers placed on three cross-sections (Figure 3a). The main axis of the dam was monitored using six vibrating-string pore pressure cells placed on three cross-sections (Figure 3b, c, d). Three further cells were placed in the foundations.

Table 1 gives the IRFA results obtained on cells and piezometers, as well as the coefficient of diffusion calculated with [22]. Twelve cell measurements were performed within a period of 451 days. The coefficient of determination ranged from 80% (cell CV33) to 96% (3 cells). Thirty-six piezometer measurements were performed within a period of 966 days. The coefficient of determination ranged in this case from 48% (piezometer P5) to 84% (3 piezometers).

Table 1. *Dam no.1, IRFA results*

Cell	α_z	η_z (days)	T (days)	L (m)	D (10^{-5} m^2/s)
Left side					
CV31	0.43	28	210	141	110
CV33	0.27	33	211	27	4
CV32	0.47	25	191	103	64
P9	0.42	45	325	111	44
P10	0.23	45	285	100	41
Middle					
CV21	0.43	56	409	140	55
CV23	0.38	33	228	32	5
CV22	0.49	33	260	106	50
P8	0.29	30	200	76	33
P3	0.21	31	193	90	49
Right side					
CV31	0.43	28	210	141	110
CV13	0.39	23	160	33	8
CV12	0.38	10	73	88	123
P7	0.28	18	119	75	55
P6	0.53	22	183	150	142
P5	0.16	91	558	107	24

The coefficient of diffusion was one order of magnitude greater in the zones located under the free surface (10^{-4} to 10^{-3} m^2/s) than in the drawdown zones (10^{-5} to 10^{-4} m^2/s). The latter were likely to be unsaturated and to have a greater hydric capacity coefficient and a lower permeability. The values (x, L) predicted from the plans of the dam showed a good match with parameter α_z identified from the monitoring data.

Despite the great difference between the principles on which the two kinds of instruments were based, the diffusivity estimates obtained with [22] were of the same order of magnitude in both cases. This consistency may be attributable to the fact that the analysis implicitly took into account the information about the whole zone

located between the upstream face and the instrument. This is larger zone than that immediately surrounding the instrument.

4.2. *Application to a zoned earthdam*

The measurements obtained on a zoned earthfill dam 42 m in height with a horizontal drainage blanket were analysed. This dam will be referred to as dam number 2. The model in [14] was used, without taking either the effects of the rainfall or those of the tailwater level into account, as they were negligible. The time effect was accounted for with the classical expression generally used in HST models.

The dam sits on a solid rock foundation, with a shallow 25 m high grout curtain placed under the central clay core. A plan of the dam and three cross sections are shown in Figure 4. Elevations are in meters above normal sea water level. A total number of 14 electrical pore pressure cells were installed on three vertical sections of the core. The data used here were obtained during a period of five years. Measurements were performed approximately every five days, and each series consisted of 355 measurements. The coefficient of determination ranged from 87% (cell CV27) to 99% (9 cells).

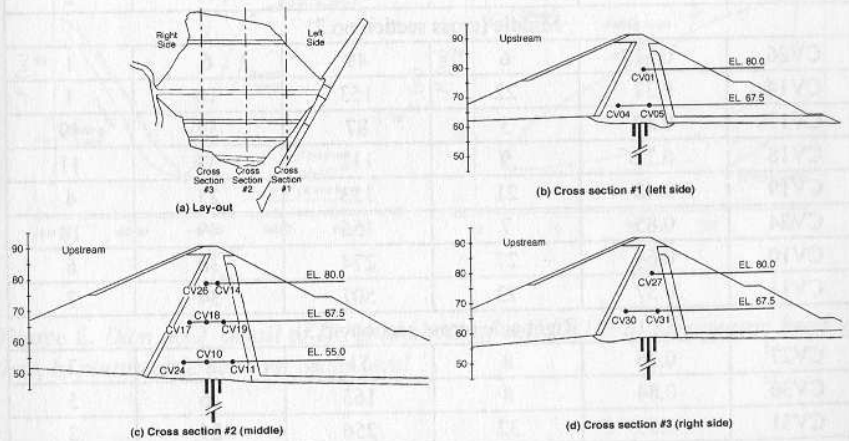

Figure 4. *Dam no.2, lay-out, cross-sections and pore-pressure cell locations*

Figure 5a gives the changes in the reservoir level and in the measured and simulated pore pressures with time at cell CV10. The reservoir level underwent a cyclic pattern of rise and fall between levels of 72 m and 86.50 m, with a period of approximately one year. An example of the loop produced by the time lag between the piezometer heads and the reservoir heads is given in Figure 5b, where the

piezometric levels are plotted as a function of the reservoir levels. The simulation obtained with the IRFA model was remarkably accurate, given the extreme simplicity of the model. This proves that the main aspects of the processes under investigation are taken into account in this model.

Figure 6 shows a typical hysteresis occurring during one increasing/decreasing water level cycle, as well as the response lag. The upper part of the loop corresponds to the first half of the cycle, while the reservoir level is falling and the piezometric head is higher than the steady state value due to the time lag. The lower part of the loop corresponds to the second half of the cycle, while the reservoir level is rising. The piezometric head is lagging, since it shows less than the steady state value.

Table 2. *Dam no.2, effects of the water level on cell data, IRFA Results*

Cell	α_Z	η_Z (days)	T (days)	L (m)	D (10^{-5} m^2/s)
Left side (cross section no.1)					
CV01	0.15	26	160	7	4
CV04	0.78	8	123	19	3
CV05	0.30	32	211	19	2
Middle (cross section no.2)					
CV26	0.51	6	49	6	1
CV14	0.37	22	153	10	1
CV17	0.89	3	87	37	19
CV18	0.72	9	112	33	11
CV19	0.42	21	153	23	4
CV24	0.85	7	156	49	18
CV10	0.64	27	274	38	6
CV11	0.37	73	507	34	3
Right side (cross section no.3)					
CV27	0.26	8	51	8	2
CV30	0.84	8	163	26	5
CV31	0.50	32	256	27	3

The results of the IRFA of the readings obtained with the 14 cells located in the core are summarized in Table 2. These results show two features: 1) the amplitude of the response α_Z decreases with the distance from the upstream face, 2) the time lag η_Z increases in the downstream direction. The distance between the cells and one of the faces of the core was estimated from the plans of the dam. The flow length L of the water path between the upstream and downstream faces (the drainage system) was also determined. The results showed a good match with parameter α_Z identified

from the monitoring data. The diffusivity of the core was found to be fairly uniform and equal to 10^{-5} m^2/s, except for a zone defined by cells CV17, CV18 and CV24 (cross section no.2), where it was ten times greater. A good knowledge of the dam would make it possible to carry out a thorough analysis.

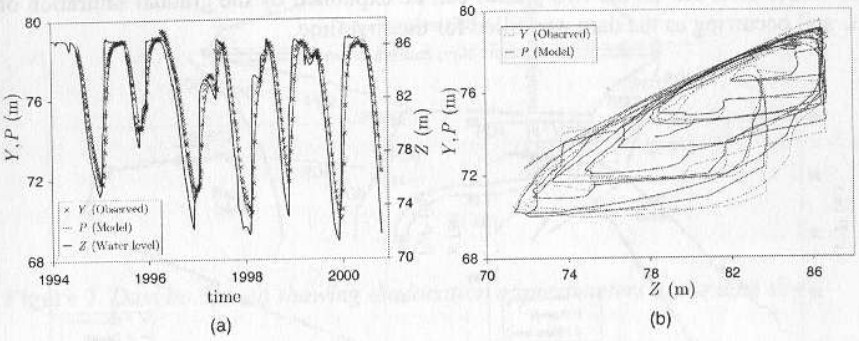

Figure 5. *Dam no.2, IRFA analysis of cellCV10: a) piezometric head vs. time, b) piezometric head vs. water level*

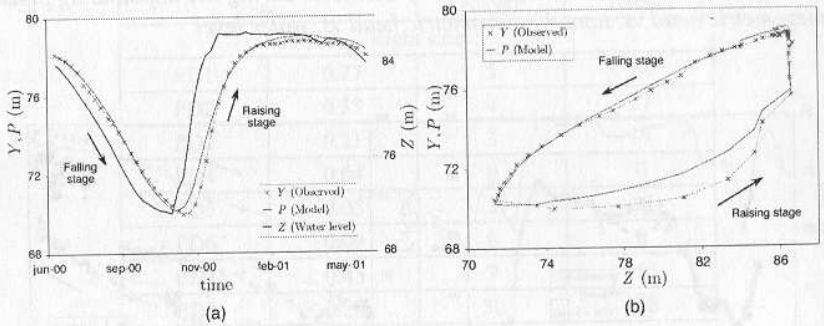

Figure 6. *Dam no.2, detail of IRFA analysis of cell CV10: a) piezometric head vs. time, b) piezometric head vs. water level*

4.3. *Application to a piezometer located downstream*

The piezometer shown in Figure 1 was installed at the downstream toe of dam no.1 (piezometer P1 in Figure 3a, b). Model [14] was used here, without taking the effects of the rainfall, the ageing, or the tailwater level into account, as they were negligible. These data were analysed in two stages. The first stage was the impounding phase. Measurements were performed approximately every day, and 120 measurements were obtained during a period of 150 days. The second stage was the first operating phase, and 570 measurements were obtained in this case during a

period of 2280 days. Fitting the IRFA model to the impoundment phase yielded $\alpha_Z = 0.44$ and $\eta_Z = 83$ days (Figure 7). The coefficient of determination was 99%. In the case of the first operating phase, we obtained $\alpha_Z = 0.22$ and $\eta_Z = 159$ days (Figure 8), and the coefficient of determination was 97%. The difference between the values obtained on the two phases can be explained by the gradual saturation of the soil occurring as the dam was filled for the first time.

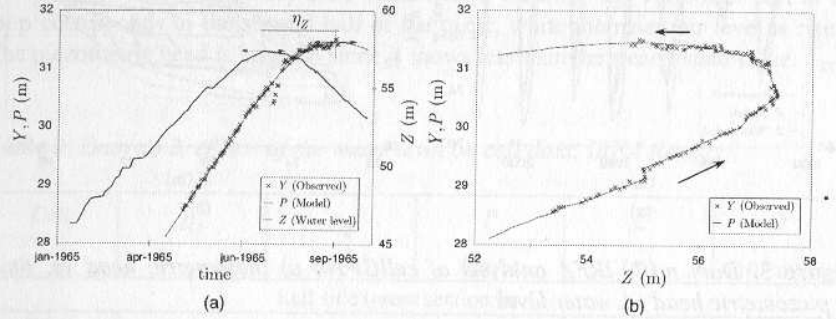

Figure 7. *Dam no.1, IRFA analysis of P1 piezometer during the impounding phase: a) piezometric head vs. time, b) piezometric head vs. water level*

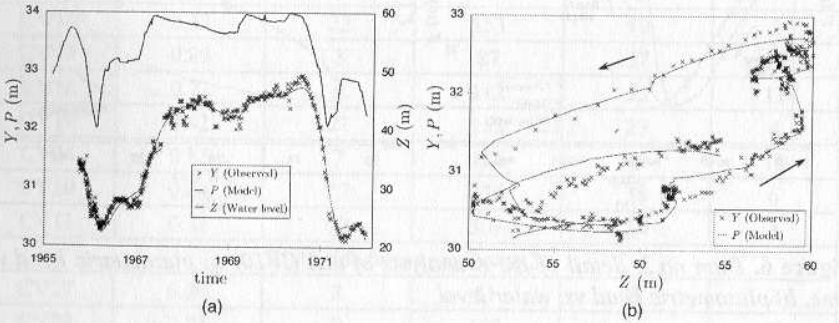

Figure 8. *Dam no.1, IRFA analysis of P1 piezometer during the exploitation phase: a) piezometric head vs. time, b) piezometric head vs. water level*

4.4. *Application to surrounding piezometers*

The monitoring data obtained on a homogeneous dam 15.5m in height were analysed. This dam will be referred to as dam no.3. The model in [14] was used, without taking the effects of the tailwater level into account. The effects of rainfall and time were included. The foundations of the dam consisted of granite with a

permeability ranging between 10^{-5} and 10^{-6} m/s, sealed off by an injected layer of sealant. Thirteen piezometers were set up around the dam (Figure 9).

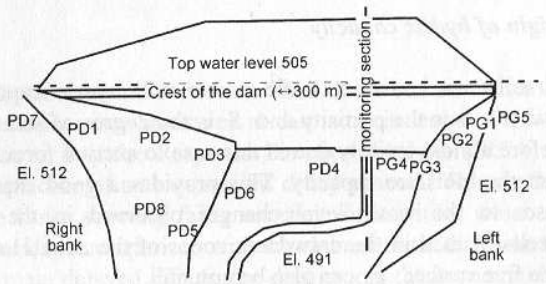

Figure 9. *Dam no.3, map showing the location of piezometers at the dam site*

Table 3. *Dam no.3, IRFA Results*

Cell	α_Z	η_Z (days)	T (days)
Right side			
PD1	0.77	5	74
PD2	0.33	4	27
PD3	0.21	3	19
PD4	0.04	0	0
PD5	0.05	3	18
PD6	0.09	0	0
PD7	0.85	7	151
PD8	0.20	30	188
Left side			
PG1	1.00	3	-
PG2	0.30	5	33
PG3	0.07	3	18
PG4	0.05	11	66
PG5	0.71	3	36

Table 3 gives the IRFA results. 107 piezometric measurements were obtained during a period of 2982 days. The coefficient of determination ranged from 64% (piezometers PG3 and PG5) to 97% (four piezometers). The effects of the reservoir level were delayed, apart from piezometers PD4 and PD6. In the case of the latter, the data had to be interpreted in the light of what was known about the dam and the foundation structures. These results show that the measurements obtained with all

the piezometers monitoring the foundations, the abutments and the surrounding banks are liable to show a time lag with respect to the actual water level.

4.5. *Possible origin of hydric capacity*

Unsaturated soils are known to have a non null hydric capacity coefficient $c_v = n\partial S / \partial p$, where n is the porosity and S is the degree of saturation. The pore pressure is therefore almost entirely due in this case to suction forces and capillaries and c_v is in fact the moisture capacity. This provides a good explanation for the delayed responses to the water level changes observed in the pore pressures measured with cells located in the drawdown zones of the dam. However, in zones located below the free surface, c_v can also be non null.

The compressibility of the soil may be an important factor, but the fine materials used to build dams usually have a low plasticity (plasticity index $I_p < 35\%$), and have been compacted. The upper layers of the dam-site are therefore over-consolidated. In addition, these materials are subjected to buoyancy forces below the free surface. The tangent stiffness modulus is therefore elastic. The contribution of the hydro-mechanical coupling to c_v is probably of the second order during the dam operation phase.

In saturated zones, the compressibility of the interstitial fluid is likely to be the most decisive factor involved. Dimensional analysis shows that $c_v = n\gamma_w / \chi_f$, where n is the porosity of the porous medium, while χ_f is the pore fluid bulk modulus and γ_w is the water density. In this case, c_v is the specific storage (Bear, 1972). St-Arnaud (1995) suggested in particular that one should take into account the fact that dam water not only has its own natural air content, but also contains air which was imprisoned when the dam was being filled, which is partly compressed and partly dissolved.

The pore fluid is a mixture of incompressible water and compressible gas bubbles. The compressibility of both solid grains and porous medium can be neglected during the dam operation phase. The bulk modulus can be shown to depend on the following factors: the initial pore pressure, the initial degree of saturation of the compacted core or the body of the dam, the current degree of saturation, the water bulk modulus and the coefficient of gas solubility (Henry's constant).

However, this analysis is not complete. Another reason for the presence of air is that the water entering the dam is saturated with air at a pressure that can differ from the atmospheric pressure (Le Bihan and Leroueil, 2000). When the water pressure increases, air is compressed (Boyle's law) and partly dissolved (Henry's law). When the water pressure decreases, air is released from the solution.

It can be concluded that the storage capacity c_v can be non-null in the so-called saturated zone, possibly because of the presence of air in the water. In this case, the interstitial pressures occurring in response to the loading will be delayed. These responses can be taken, however, to be instantaneous responses at characteristic

times shorter than the response times of the monitoring devices and the measuring rates used here.

5. Conclusion

No practical, efficient methods have been described so far in the literature for analysing the pore pressures measured at dam sites in terms of the reservoir levels. Here we propose an Impulse Response Function Analysis (IRFA) method dealing with the particular case of an exponential decay process. This model is appropriate for dealing with flows showing fairly constant diffusivities, which are subjected to slowly varying loads in comparison with the characteristic diffusion time. It accounts for some of the main delayed effects: the dissipation, the accommodation (delay and damping) under cyclic loading, and the influence of the past loading history.

The present analysis of monitoring data obtained at three dams showed that the measurements obtained with all the instruments tested, including pore pressure cells placed in the body of the dam and piezometers monitoring the body of the dam, the foundations, the abutments and the surrounding banks, were liable to show time lags with respect to the actual water level. The characteristic diffusion times were found to range between a few days and a few months.

The IRFA method depends to a large extent on the Green's function. This makes the model mechanically relevant, because of the temporal moment method used. It is possible in particular with this method to obtain hydraulic diffusivity estimates on the body of the dam, which ranged in the present cases studies between 10^{-6} and 10^{-3} m^2/s. This information can be used to check the effects of structural defects and the ageing of the dam, or to assess the effectiveness of repair works, by comparing the values identified before and after interventions.

6. References

Bear J., *Dynamics of Fluids in Porous Media*. Dover, New York, 1972.

Beck J. V., Cole K. D., Haji-Sheikh A., Litkouhi B., *Heat Conduction Using Green's Functions*, Hemisphere, Washington, DC, 1992.

Bonelli S., Félix H., Tourment R., « Interprétation des mesures d'auscultation des barrages par régression linéaire multiple HST », *Fiabilité des matériaux et des structures*, Hermès, 1998, p. 188-198.

Carrère A., Colson M., Goguel B., Noret C., "Modelling: a means of assisting interpretation of readings", *XX^th International Congress on Large Dams*, Beijing, ICOLD, 2000, p. 1005-1037.

Delay F., Porel G., Banton O., "An approach to transport in heterogeneous porous media using the truncated temporal moment equations: theory and numerical validation", *Transport in Porous Media*, vol. 32, 1998, p. 199-232.

Ferry S., Willm G., « Méthodes d'analyse et de surveillance des déplacements observés par le moyen de pendules dans les barrages », *VI^th International Congress on Large Dams*, New-York, ICOLD, 1958, p.1179-1201.

Forbes J. D., "Account of some experiments on the temperature of the earth at different depths and in different soils near Edinburgh", *Transactions of The Royal Society of Edinburgh*, vol. 16, 1846, p. 189-236.

Goltz M. N., Roberts P. V., "Using the method of moments to analyze three-dimensional diffusion-limited solute transport from temporal and spatial perspectives", *Water Resources Research*, vol. 23, 1987, p. 1757-1585.

Gradshtein I. S., *Table of Integrals, Series and Products*, Academic Press, New York, 1980.

Guedes Q. M., Coelho P. S. M., "Statistical behaviour model of dams", *XV^th International Congress on Large Dams*, Lausanne, ICOLD, 1985, p. 319-334.

Kjaernsli B., Kvale G., Lunde J., Baade-Mathiesen J., "Design, construction, control and performance of the Svartevann earth-rockfill dam", *XIV^th International Congress on Large Dams*, Rio de Janeiro, ICOLD, 1982, p. 319-349.

Le Bihan J.-P., Leroueil S., "A model for gas and water through the core of earth dams", *Canadian Geotechnical Journal*, vol. 39, 2002, p. 90-102.

Melnikov Yu. A., "An alternative construction of Green's functions for the two-dimensional heat equation", *Engineering Analysis with Boundary Elements*, vol. 24, 2000, p. 467-475.

Morse P. M., Feshbach H., *Methods of Theoretical Physics: Parts I and II*, New York, McGraw-Hill, 1953.

Myrvoll F., Larsen S., Sande A., Romsol N. B., "Field instrumentation and performance observations for the Vatnedalsvatn dams", *XV^th International Congress on Large Dams*, Lausanne, ICOLD, 1985, p. 1039-1069.

Roach G. F., *Green's functions, introductory theory with applications*, Van Nostrand Reinhold Company, 1970.

Silva Gomes A. F., Silva Matos D., "Quantitative analysis of dam monitoring results, state of the art, applications and prospects", *XV^th International Congress on Large Dams*, Lausanne, ICOLD, 1985, p. 749-761.

St-Arnaud G., "The high pore pressures within embankment dams: an unsaturated soil approach", *Canadian Geotechnical Journal*, vol. 32, 1995, p. 892-898.

Willm G., Beaujoint N., « Les méthodes de surveillance des barrages au service de la production hydraulique d'Electricité de France, problèmes anciens et solutions nouvelles », *IX^th International Congress on Large Dams*, Istanbul, ICOLD, 1967, p. 529-550.

Windisch E., Høeg K., "Pore pressure in the till core of Oddatjorn dam", *53^rd Canadian Geotechnical Conference*, Montreal, 2000, p. 231-238.

Young P., "Data-based mechanistic modelling of environmental, ecological, economic and engineering systems", *Environmental Modelling & Software*, vol. 13, 1998, p. 105-122.

Received : 21 November 2006
Accepted : 27 September 2007

Numerical modelling of geocomposite cells designed for rockfall protection

David Bertrand

Cemagref, Groupement de Grenoble - Domaine universitaire
2, rue de la Papeterie, BP 76
F-38402 Saint-Martin-d'Hères cedex

david.bertrand@grenoble.cemagref.fr

ABSTRACT. *This study investigated rockfall protection barriers built with cell assembly. This structure was modelled using a multiscale approach where the cell scale and the barrier scale were distinguished. This paper focuses on the cell modelling. Cells are composed of a granular media surrounded by a wire mesh. The medium is described using the discrete element method, which is well suited to simulating its granular nature. The numerical model was calibrated and validated by comparing the simulation results to experimental data from mechanical tests on 500-mm cube-like cells. These tests were conducted in quasi-static condition and dynamic condition. The numerical results were in agreement with the experimental results.*

RÉSUMÉ. *L'étude porte sur des structures de protection contre les chutes de bloc à technologie cellulaire. Ce type d'ouvrage fait l'objet d'une modélisation multi-échelle où l'on distingue l'échelle de la cellule de celle de l'ouvrage. Cet article présente la modélisation numérique de cellules remplies de pierres entourées par un grillage métallique à maille hexagonale. La description du matériau granulaire est réalisée à partir d'une approche numérique discrète adaptée pour simuler sa granularité. Le calage et la validation du modèle numérique sont effectués en comparant les résultats des simulations numériques à des essais expérimentaux réalisés sur des cellules cubiques de 500 mm de côté dans des conditions quasi statique et dynamique d'impact. Les résultats numériques sont en accord avec les expérimentations.*

KEYWORDS: *discrete numerical simulation, rockfalls, cellular structure, wire mesh.*

MOTS-CLÉS : *modélisation numérique discrète, chutes de blocs, structure cellulaire, grillage.*

DOI:10.3166/EJECE.12.263-277 © 2008 Lavoisier, Paris